

# Measurement of the integrated luminosities of the data taken by BESIII at $\sqrt{s} = 3.650$ and $3.773$ GeV \*

M. Ablikim<sup>1</sup>, M. N. Achasov<sup>7,a</sup>, O. Albayrak<sup>4</sup>, D. J. Ambrose<sup>40</sup>, F. F. An<sup>1</sup>, Q. An<sup>41</sup>, J. Z. Bai<sup>1</sup>, R. Baldini Ferroli<sup>18A</sup>,  
Y. Ban<sup>27</sup>, J. Becker<sup>3</sup>, J. V. Bennett<sup>17</sup>, M. Bertani<sup>18A</sup>, J. M. Bian<sup>39</sup>, E. Boger<sup>20,b</sup>, O. Bondarenko<sup>21</sup>, I. Boyko<sup>20</sup>,  
R. A. Briere<sup>4</sup>, V. Bytev<sup>20</sup>, H. Cai<sup>45</sup>, X. Cai<sup>1</sup>, O. Cakir<sup>35A</sup>, A. Calcaterra<sup>18A</sup>, G. F. Cao<sup>1</sup>, S. A. Cetin<sup>35B</sup>, J. F. Chang<sup>1</sup>,  
G. Chelkov<sup>20,b</sup>, G. Chen<sup>1</sup>, H. S. Chen<sup>1</sup>, J. C. Chen<sup>1</sup>, M. L. Chen<sup>1</sup>, S. J. Chen<sup>25</sup>, X. Chen<sup>27</sup>, X. R. Chen<sup>22</sup>, Y. B. Chen<sup>1</sup>,  
H. P. Cheng<sup>15</sup>, Y. P. Chu<sup>1</sup>, D. Cronin-Hennessy<sup>39</sup>, H. L. Dai<sup>1</sup>, J. P. Dai<sup>1</sup>, D. Dedovich<sup>20</sup>, Z. Y. Deng<sup>1</sup>, A. Denig<sup>19</sup>,  
I. Denysenko<sup>20</sup>, M. Destefanis<sup>44A,44C</sup>, W. M. Ding<sup>29</sup>, Y. Ding<sup>23</sup>, L. Y. Dong<sup>1</sup>, M. Y. Dong<sup>1</sup>, S. X. Du<sup>47</sup>, J. Fang<sup>1</sup>,  
S. S. Fang<sup>1</sup>, L. Fava<sup>44B,44C</sup>, C. Q. Feng<sup>41</sup>, P. Friedel<sup>3</sup>, C. D. Fu<sup>1</sup>, J. L. Fu<sup>25</sup>, O. Fuks<sup>20,b</sup>, Y. Gao<sup>34</sup>, C. Geng<sup>41</sup>, K. Goetzen<sup>8</sup>,  
W. X. Gong<sup>1</sup>, W. Gradl<sup>19</sup>, M. Greco<sup>44A,44C</sup>, M. H. Gu<sup>1</sup>, Y. T. Gu<sup>10</sup>, Y. H. Guan<sup>37</sup>, A. Q. Guo<sup>26</sup>, L. B. Guo<sup>24</sup>, T. Guo<sup>24</sup>,  
Y. P. Guo<sup>26</sup>, Y. L. Han<sup>1</sup>, F. A. Harris<sup>38</sup>, K. L. He<sup>1</sup>, M. He<sup>1</sup>, Z. Y. He<sup>26</sup>, T. Held<sup>3</sup>, Y. K. Heng<sup>1</sup>, Z. L. Hou<sup>1</sup>, C. Hu<sup>24</sup>,  
H. M. Hu<sup>1</sup>, J. F. Hu<sup>36</sup>, T. Hu<sup>1</sup>, G. M. Huang<sup>5</sup>, G. S. Huang<sup>41</sup>, J. S. Huang<sup>13</sup>, L. Huang<sup>1</sup>, X. T. Huang<sup>29</sup>, Y. Huang<sup>25</sup>,  
T. Hussain<sup>43</sup>, C. S. Ji<sup>41</sup>, Q. Ji<sup>1</sup>, Q. P. Ji<sup>26</sup>, X. B. Ji<sup>1</sup>, X. L. Ji<sup>1</sup>, L. L. Jiang<sup>1</sup>, X. S. Jiang<sup>1</sup>, J. B. Jiao<sup>29</sup>, Z. Jiao<sup>15</sup>, D. P. Jin<sup>1</sup>,  
S. Jin<sup>1</sup>, F. F. Jing<sup>34</sup>, N. Kalantar-Nayestanaki<sup>21</sup>, M. Kavatsyuk<sup>21</sup>, Kloss<sup>19</sup>, B. Kopf<sup>3</sup>, M. Kornicer<sup>38</sup>, W. Kuehn<sup>36</sup>, W. Lai<sup>1</sup>,  
J. S. Lange<sup>36</sup>, M. Lara<sup>17</sup>, P. Larin<sup>12</sup>, M. Leyhe<sup>3</sup>, C. H. Li<sup>1</sup>, Cheng Li<sup>41</sup>, Cui Li<sup>41</sup>, D. M. Li<sup>47</sup>, F. Li<sup>1</sup>, G. Li<sup>1</sup>, H. B. Li<sup>1</sup>,  
J. C. Li<sup>1</sup>, K. Li<sup>11</sup>, Lei Li<sup>1</sup>, Q. J. Li<sup>1</sup>, S. L. Li<sup>1</sup>, W. D. Li<sup>1</sup>, W. G. Li<sup>1</sup>, X. L. Li<sup>29</sup>, X. N. Li<sup>1</sup>, X. Q. Li<sup>26</sup>, X. R. Li<sup>28</sup>, Z. B. Li<sup>33</sup>,  
H. Liang<sup>41</sup>, Y. F. Liang<sup>31</sup>, Y. T. Liang<sup>36</sup>, G. R. Liao<sup>34</sup>, X. T. Liao<sup>1</sup>, D. Lin<sup>12</sup>, B. J. Liu<sup>1</sup>, C. L. Liu<sup>4</sup>, C. X. Liu<sup>1</sup>, F. H. Liu<sup>30</sup>,  
Fang Liu<sup>1</sup>, Feng Liu<sup>5</sup>, H. Liu<sup>1</sup>, H. B. Liu<sup>10</sup>, H. H. Liu<sup>14</sup>, H. M. Liu<sup>1</sup>, H. W. Liu<sup>1</sup>, J. P. Liu<sup>45</sup>, K. Liu<sup>34</sup>, K. Y. Liu<sup>23</sup>,  
P. L. Liu<sup>29</sup>, Q. Liu<sup>37</sup>, S. B. Liu<sup>41</sup>, X. Liu<sup>22</sup>, Y. B. Liu<sup>26</sup>, Z. A. Liu<sup>1</sup>, Zhiqiang Liu<sup>1</sup>, Zhiqing Liu<sup>1</sup>, H. Loehner<sup>21</sup>, X. C. Lou<sup>1,c</sup>,  
G. R. Lu<sup>13</sup>, H. J. Lu<sup>15</sup>, J. G. Lu<sup>1</sup>, X. R. Lu<sup>37</sup>, Y. P. Lu<sup>1</sup>, C. L. Luo<sup>24</sup>, M. X. Luo<sup>46</sup>, T. Luo<sup>38</sup>, X. L. Luo<sup>1</sup>, M. Lv<sup>1</sup>,  
C. L. Ma<sup>37</sup>, F. C. Ma<sup>23</sup>, H. L. Ma<sup>1</sup>, Q. M. Ma<sup>1</sup>, S. Ma<sup>1</sup>, T. Ma<sup>1</sup>, X. Y. Ma<sup>1</sup>, F. E. Maas<sup>12</sup>, M. Maggiora<sup>44A,44C</sup>,  
Q. A. Malik<sup>43</sup>, Y. J. Mao<sup>27</sup>, Z. P. Mao<sup>1</sup>, J. G. Messchendorp<sup>21</sup>, J. Min<sup>1</sup>, T. J. Min<sup>1</sup>, R. E. Mitchell<sup>17</sup>, X. H. Mo<sup>1</sup>,  
H. Moeini<sup>21</sup>, C. Morales Morales<sup>12</sup>, K. Moriya<sup>17</sup>, N. Yu. Muchnoi<sup>7,a</sup>, H. Muramatsu<sup>40</sup>, Y. Nefedov<sup>20</sup>, C. Nicholson<sup>37</sup>,  
I. B. Nikolaev<sup>7,a</sup>, Z. Ning<sup>1</sup>, S. L. Olsen<sup>28</sup>, Q. Ouyang<sup>1</sup>, S. Pacetti<sup>18B</sup>, J. W. Park<sup>38</sup>, M. Pelizaeus<sup>3</sup>, H. P. Peng<sup>41</sup>, K. Peters<sup>8</sup>,  
J. L. Ping<sup>24</sup>, R. G. Ping<sup>1</sup>, R. Poling<sup>39</sup>, E. Prencipe<sup>19</sup>, M. Qi<sup>25</sup>, S. Qian<sup>1</sup>, C. F. Qiao<sup>37</sup>, L. Q. Qin<sup>29</sup>, X. S. Qin<sup>1</sup>, Y. Qin<sup>27</sup>,  
Z. H. Qin<sup>1</sup>, J. F. Qiu<sup>1</sup>, K. H. Rashid<sup>43</sup>, G. Rong<sup>1</sup>, X. D. Ruan<sup>10</sup>, A. Sarantsev<sup>20,d</sup>, M. Shao<sup>41</sup>, C. P. Shen<sup>2</sup>, X. Y. Shen<sup>1</sup>,  
H. Y. Sheng<sup>1</sup>, M. R. Shepherd<sup>17</sup>, W. M. Song<sup>1</sup>, X. Y. Song<sup>1</sup>, S. Spataro<sup>44A,44C</sup>, B. Spruck<sup>36</sup>, D. H. Sun<sup>1</sup>, G. X. Sun<sup>1</sup>,  
J. F. Sun<sup>13</sup>, S. S. Sun<sup>1</sup>, Y. J. Sun<sup>41</sup>, Y. Z. Sun<sup>1</sup>, Z. J. Sun<sup>1</sup>, Z. T. Sun<sup>41</sup>, C. J. Tang<sup>31</sup>, X. Tang<sup>1</sup>, I. Tapan<sup>35C</sup>,  
E. H. Thorndike<sup>40</sup>, D. Toth<sup>39</sup>, M. Ullrich<sup>36</sup>, I. Uman<sup>35B</sup>, G. S. Varner<sup>38</sup>, B. Wang<sup>1</sup>, D. Wang<sup>27</sup>, D. Y. Wang<sup>27</sup>, K. Wang<sup>1</sup>,  
L. L. Wang<sup>1</sup>, L. S. Wang<sup>1</sup>, M. Wang<sup>29</sup>, P. Wang<sup>1</sup>, P. L. Wang<sup>1</sup>, Q. J. Wang<sup>1</sup>, S. G. Wang<sup>27</sup>, X. F. Wang<sup>34</sup>, X. L. Wang<sup>41</sup>,  
Y. D. Wang<sup>18A</sup>, Y. F. Wang<sup>1</sup>, Y. Q. Wang<sup>19</sup>, Z. Wang<sup>1</sup>, Z. G. Wang<sup>1</sup>, Z. Y. Wang<sup>1</sup>, D. H. Wei<sup>9</sup>, J. B. Wei<sup>27</sup>,  
P. Weidenkaff<sup>19</sup>, Q. G. Wen<sup>41</sup>, S. P. Wen<sup>1</sup>, M. Werner<sup>36</sup>, U. Wiedner<sup>3</sup>, L. H. Wu<sup>1</sup>, N. Wu<sup>1</sup>, S. X. Wu<sup>41</sup>, W. Wu<sup>26</sup>, Z. Wu<sup>1</sup>,  
L. G. Xia<sup>34</sup>, Y. X. Xia<sup>16</sup>, Z. J. Xiao<sup>24</sup>, Y. G. Xie<sup>1</sup>, Q. L. Xiu<sup>1</sup>, G. F. Xu<sup>1</sup>, G. M. Xu<sup>27</sup>, Q. J. Xu<sup>11</sup>, Q. N. Xu<sup>37</sup>, X. P. Xu<sup>32</sup>,  
Z. R. Xu<sup>41</sup>, Z. Xue<sup>1</sup>, L. Yan<sup>41</sup>, W. B. Yan<sup>41</sup>, Y. H. Yan<sup>16</sup>, H. X. Yang<sup>1</sup>, Y. Yang<sup>5</sup>, Y. X. Yang<sup>9</sup>, H. Ye<sup>1</sup>, M. Ye<sup>1</sup>, M. H. Ye<sup>6</sup>,  
B. X. Yu<sup>1</sup>, C. X. Yu<sup>26</sup>, H. W. Yu<sup>27</sup>, J. S. Yu<sup>22</sup>, S. P. Yu<sup>29</sup>, C. Z. Yuan<sup>1</sup>, Y. Yuan<sup>1</sup>, A. A. Zafar<sup>43</sup>, A. Zallo<sup>18A</sup>, S. L. Zhang<sup>25</sup>,  
Y. Zeng<sup>16</sup>, B. X. Zhang<sup>1</sup>, B. Y. Zhang<sup>1</sup>, C. Zhang<sup>25</sup>, C. C. Zhang<sup>1</sup>, D. H. Zhang<sup>1</sup>, H. H. Zhang<sup>33</sup>, H. Y. Zhang<sup>1</sup>,  
J. Q. Zhang<sup>1</sup>, J. W. Zhang<sup>1</sup>, J. Y. Zhang<sup>1</sup>, J. Z. Zhang<sup>1</sup>, LiLi Zhang<sup>16</sup>, R. Zhang<sup>37</sup>, S. H. Zhang<sup>1</sup>, X. J. Zhang<sup>1</sup>,  
X. Y. Zhang<sup>29</sup>, Y. Zhang<sup>1</sup>, Y. H. Zhang<sup>1</sup>, Z. P. Zhang<sup>41</sup>, Z. Y. Zhang<sup>45</sup>, Zhenghao Zhang<sup>5</sup>, G. Zhao<sup>1</sup>, H. S. Zhao<sup>1</sup>,  
J. W. Zhao<sup>1</sup>, K. X. Zhao<sup>24</sup>, Lei Zhao<sup>41</sup>, Ling Zhao<sup>1</sup>, M. G. Zhao<sup>26</sup>, Q. Zhao<sup>1</sup>, S. J. Zhao<sup>47</sup>, T. C. Zhao<sup>1</sup>, X. H. Zhao<sup>25</sup>,  
Y. B. Zhao<sup>1</sup>, Z. G. Zhao<sup>41</sup>, A. Zhemchugov<sup>20,b</sup>, B. Zheng<sup>42</sup>, J. P. Zheng<sup>1</sup>, Y. H. Zheng<sup>37</sup>, B. Zhong<sup>24</sup>, L. Zhou<sup>1</sup>, X. Zhou<sup>45</sup>,  
X. K. Zhou<sup>37</sup>, X. R. Zhou<sup>41</sup>, C. Zhu<sup>1</sup>, K. Zhu<sup>1</sup>, K. J. Zhu<sup>1</sup>, S. H. Zhu<sup>1</sup>, X. L. Zhu<sup>34</sup>, Y. C. Zhu<sup>41</sup>, Y. M. Zhu<sup>26</sup>, Y. S. Zhu<sup>1</sup>,  
Z. A. Zhu<sup>1</sup>, J. Zhuang<sup>1</sup>, B. S. Zou<sup>1</sup>, J. H. Zou<sup>1</sup>

(BESIII Collaboration)

<sup>1</sup> Institute of High Energy Physics, Beijing 100049, People's Republic of China

\* Supported in part by the Ministry of Science and Technology of China under Contract No. 2009CB825200; National Natural Science Foundation of China (NSFC) under Contracts Nos. 10625524, 10821063, 10825524, 10835001, 10935007, 11125525, 11235011; Joint Funds of the National Natural Science Foundation of China under Contracts Nos. 11079008, 11179007; the Chinese Academy of Sciences (CAS) Large-Scale Scientific Facility Program; CAS under Contracts Nos. KJCX2-YW-N29, KJCX2-YW-N45; 100 Talents Program of CAS; German Research Foundation DFG under Contract No. Collaborative Research Center CRC-1044; Istituto Nazionale di Fisica Nucleare, Italy; Ministry of Development of Turkey under Contract No. DPT2006K-120470; U. S. Department of Energy under Contracts Nos. DE-FG02-04ER41291, DE-FG02-05ER41374, DE-FG02-94ER40823; U.S. National Science Foundation; University of Groningen (RuG) and the Helmholtzzentrum fuer Schwerionenforschung GmbH (GSI), Darmstadt; WCU Program of National Research Foundation of Korea under Contract No. R32-2008-000-10155-0.

- 
- <sup>2</sup> *Beihang University, Beijing 100191, People's Republic of China*  
<sup>3</sup> *Bochum Ruhr-University, D-44780 Bochum, Germany*  
<sup>4</sup> *Carnegie Mellon University, Pittsburgh, Pennsylvania 15213, USA*  
<sup>5</sup> *Central China Normal University, Wuhan 430079, People's Republic of China*  
<sup>6</sup> *China Center of Advanced Science and Technology, Beijing 100190, People's Republic of China*  
<sup>7</sup> *G.I. Budker Institute of Nuclear Physics SB RAS (BINP), Novosibirsk 630090, Russia*  
<sup>8</sup> *GSI Helmholtzcentre for Heavy Ion Research GmbH, D-64291 Darmstadt, Germany*  
<sup>9</sup> *Guangxi Normal University, Guilin 541004, People's Republic of China*  
<sup>10</sup> *GuangXi University, Nanning 530004, People's Republic of China*  
<sup>11</sup> *Hangzhou Normal University, Hangzhou 310036, People's Republic of China*  
<sup>12</sup> *Helmholtz Institute Mainz, Johann-Joachim-Becher-Weg 45, D-55099 Mainz, Germany*  
<sup>13</sup> *Henan Normal University, Xinxiang 453007, People's Republic of China*  
<sup>14</sup> *Henan University of Science and Technology, Luoyang 471003, People's Republic of China*  
<sup>15</sup> *Huangshan College, Huangshan 245000, People's Republic of China*  
<sup>16</sup> *Hunan University, Changsha 410082, People's Republic of China*  
<sup>17</sup> *Indiana University, Bloomington, Indiana 47405, USA*  
<sup>18</sup> *(A)INFN Laboratori Nazionali di Frascati, I-00044, Frascati, Italy; (B)INFN and University of Perugia, I-06100, Perugia, Italy*  
<sup>19</sup> *Johannes Gutenberg University of Mainz, Johann-Joachim-Becher-Weg 45, D-55099 Mainz, Germany*  
<sup>20</sup> *Joint Institute for Nuclear Research, 141980 Dubna, Moscow region, Russia*  
<sup>21</sup> *KVI, University of Groningen, NL-9747 AA Groningen, The Netherlands*  
<sup>22</sup> *Lanzhou University, Lanzhou 730000, People's Republic of China*  
<sup>23</sup> *Liaoning University, Shenyang 110036, People's Republic of China*  
<sup>24</sup> *Nanjing Normal University, Nanjing 210023, People's Republic of China*  
<sup>25</sup> *Nanjing University, Nanjing 210093, People's Republic of China*  
<sup>26</sup> *Nankai university, Tianjin 300071, People's Republic of China*  
<sup>27</sup> *Peking University, Beijing 100871, People's Republic of China*  
<sup>28</sup> *Seoul National University, Seoul, 151-747 Korea*  
<sup>29</sup> *Shandong University, Jinan 250100, People's Republic of China*  
<sup>30</sup> *Shanxi University, Taiyuan 030006, People's Republic of China*  
<sup>31</sup> *Sichuan University, Chengdu 610064, People's Republic of China*  
<sup>32</sup> *Soochow University, Suzhou 215006, People's Republic of China*  
<sup>33</sup> *Sun Yat-Sen University, Guangzhou 510275, People's Republic of China*  
<sup>34</sup> *Tsinghua University, Beijing 100084, People's Republic of China*  
<sup>35</sup> *(A)Ankara University, Dogol Caddesi, 06100 Tandogan, Ankara, Turkey; (B)Dogus University, 34722 Istanbul, Turkey; (C)Uludag University, 16059 Bursa, Turkey*  
<sup>36</sup> *Universitaet Giessen, D-35392 Giessen, Germany*  
<sup>37</sup> *University of Chinese Academy of Sciences, Beijing 100049, People's Republic of China*  
<sup>38</sup> *University of Hawaii, Honolulu, Hawaii 96822, USA*  
<sup>39</sup> *University of Minnesota, Minneapolis, Minnesota 55455, USA*  
<sup>40</sup> *University of Rochester, Rochester, New York 14627, USA*  
<sup>41</sup> *University of Science and Technology of China, Hefei 230026, People's Republic of China*  
<sup>42</sup> *University of South China, Hengyang 421001, People's Republic of China*  
<sup>43</sup> *University of the Punjab, Lahore-54590, Pakistan*  
<sup>44</sup> *(A)University of Turin, I-10125, Turin, Italy; (B)University of Eastern Piedmont, I-15121, Alessandria, Italy; (C)INFN, I-10125, Turin, Italy*  
<sup>45</sup> *Wuhan University, Wuhan 430072, People's Republic of China*  
<sup>46</sup> *Zhejiang University, Hangzhou 310027, People's Republic of China*  
<sup>47</sup> *Zhengzhou University, Zhengzhou 450001, People's Republic of China*  
<sup>a</sup> *Also at the Novosibirsk State University, Novosibirsk, 630090, Russia*  
<sup>b</sup> *Also at the Moscow Institute of Physics and Technology, Moscow 141700, Russia*  
<sup>c</sup> *Also at University of Texas at Dallas, Richardson, Texas 75083, USA*  
<sup>d</sup> *Also at the PNPI, Gatchina 188300, Russia*

**Abstract:**

Data sets were collected with the BESIII detector at the BEPCII collider at the center-of-mass energy of  $\sqrt{s} = 3.650$  GeV during May 2009 and at  $\sqrt{s} = 3.773$  GeV from January 2010 to May 2011. By analyzing the large angle Bhabha

scattering events, the integrated luminosities of the two data sets are measured to be  $(44.49 \pm 0.02 \pm 0.44) \text{ pb}^{-1}$  and  $(2916.94 \pm 0.18 \pm 29.17) \text{ pb}^{-1}$ , respectively, where the first error is statistical and the second error is systematic.

**Key words:** Bhabha scattering events, integrated luminosity, cross section

**PACS:** 11.30.Rd, 13.66.Bc

## 1 Introduction

In  $e^+e^-$  collider experiments, the number of events for  $e^+e^- \rightarrow X$  observed in a data set can be written as

$$N_{e^+e^- \rightarrow X}^{\text{obs}}(\sqrt{s}) = L(\sqrt{s}) \times \epsilon_{e^+e^- \rightarrow X}(\sqrt{s}) \times \sigma^{\text{obs}}(\sqrt{s}), \quad (1)$$

where  $X$  denotes some final state produced in  $e^+e^-$  annihilation,  $N_{e^+e^- \rightarrow X}^{\text{obs}}$  is the number of events observed,  $\epsilon_{e^+e^- \rightarrow X}$  is the detection efficiency for  $e^+e^- \rightarrow X$ ,  $L$  is the integrated luminosity and  $\sqrt{s}$  is the center-of-mass energy.

To systematically study the properties of the production and decays of  $\psi(3770)$  and  $D$  mesons, a data set was taken at  $\sqrt{s} = 3.773 \text{ GeV}$ , with the BESIII detector at the BEPCII, from January 2010 to May 2011. So far, this data set is the largest  $e^+e^-$  collision data set taken around the  $\psi(3770)$  resonance peak in the world. In order to estimate the continuum contribution in the studies of the resonance decays, another data set was taken in 2009 at  $\sqrt{s} = 3.650 \text{ GeV}$ , which is far away from the resonance peak. The data taken at  $\sqrt{s} = 3.773 \text{ GeV}$  was accumulated in different periods of BESIII running; the first part was taken from January 2010 to June 2010 and the second part was taken from December 2010 to May 2011. For convenience in the following, we call the data taken at  $\sqrt{s} = 3.650 \text{ GeV}$  as the continuum data and call the two parts of the data taken at  $\sqrt{s} = 3.773 \text{ GeV}$  as  $\psi(3770)$  data A and  $\psi(3770)$  data B, respectively.

In this paper, we present the measurements of the integrated luminosities of the data sets taken at  $\sqrt{s} = 3.650$  and  $3.773 \text{ GeV}$  by analyzing the large angle Bhabha scattering events.

## 2 BESIII detector

The BESIII detector and the BEPCII collider [1] are major upgrades of the BESII detector and the BEPC collider [2]. The design peak luminosity of the double-ring  $e^+e^-$  collider, BEPCII, is  $10^{33} \text{ cm}^{-2}\text{s}^{-1}$  at a beam current of 0.93 A. The peak luminosity at  $\sqrt{s} = 3.773 \text{ GeV}$  reached  $0.65 \times 10^{33} \text{ cm}^{-2}\text{s}^{-1}$  in April 2011 during the  $\psi(3770)$  data taking. The BESIII detector with a geometrical acceptance of 93% of  $4\pi$ , consists of the following main components: 1) a small-celled, helium-based main draft chamber (MDC) with 43 layers. The average

single wire resolution is  $135 \mu\text{m}$ , and the momentum resolution for  $1 \text{ GeV}/c$  charged particles in a 1 T magnetic field is 0.5%; 2) an electromagnetic calorimeter (EMC) made of 6240 CsI (Tl) crystals arranged in a cylindrical shape (barrel) plus two endcaps. For 1.0 GeV photons, the energy resolution is 2.5% in the barrel and 5% in the endcaps, and the position resolution is 6 mm in the barrel and 9 mm in the endcaps; 3) a Time-Of-Flight system (TOF) for particle identification composed of a barrel part made of two layers with 88 pieces of 5 cm thick, 2.4 m long plastic scintillator in each layer, and two endcaps with 96 fan-shaped, 5 cm thick, plastic scintillators in each endcap. The time resolution is 80 ps in the barrel, and 110 ps in the endcaps, corresponding to a  $2\sigma \text{ K}/\pi$  separation for momenta up to about  $1.0 \text{ GeV}/c$ ; 4) a muon chamber system (MUC) made of 1600  $\text{m}^2$  of Resistive Plate Chambers (RPC) arranged in 9 layers in the barrel and 8 layers in the endcaps and incorporated in the return iron of the superconducting magnet. The position resolution is about 2 cm.

## 3 Method

In principle, any QED process can be used to measure the integrated luminosity of the data set using

$$L(\sqrt{s}) = \frac{N_{\text{QED}}^{\text{obs}}(\sqrt{s}) \times (1 - \eta)}{\sigma_{\text{QED}}(\sqrt{s}) \times \epsilon \times \epsilon_{e^+e^-}^{\text{trig}}}, \quad (2)$$

where  $N_{\text{QED}}^{\text{obs}}$  is the observed number of events of the final state in question,  $\sigma_{\text{QED}}$  is the production cross section, which can be determined by theoretical calculation,  $\epsilon$  is the detection efficiency,  $\eta$  is the contamination ratio and  $\epsilon_{e^+e^-}^{\text{trig}}$  is the trigger efficiency for collecting the QED process in the on-line data acquisition.

Usually, the processes of  $e^+e^- \rightarrow (\gamma)e^+e^-$ ,  $e^+e^- \rightarrow (\gamma)\gamma\gamma$  and  $e^+e^- \rightarrow (\gamma)\mu^+\mu^-$  are used to measure the integrated luminosity of the data because of their simpler final state topologies, larger production cross sections, higher detection efficiencies, as well as more precisely expected cross sections from theory. In this work, the large angle Bhabha scattering events of  $e^+e^- \rightarrow (\gamma)e^+e^-$  are adopted. Throughout the paper, the symbol of “ $(\gamma)$ ” denotes the possible photon(s) produced due to Initial State Radiation or Final State Radiation.

## 4 Luminosity measurement

### 4.1 Event selection

In order to select candidate Bhabha events, it is required that there should be only two good charged tracks with total charge zero, which are reconstructed in the MDC. Each track must originate from the interaction region of  $R_{xy} < 1$  cm and  $|V_z| < 5$  cm, where  $R_{xy}$  and  $|V_z|$  are the points of closest approach relative to the collision point in the xy-plane and in the z direction, respectively. Furthermore, to ensure that the candidate charged track hits the barrel of the EMC, we require that the polar angle  $\theta$  of the charged track satisfy  $|\cos\theta| < 0.80$ .

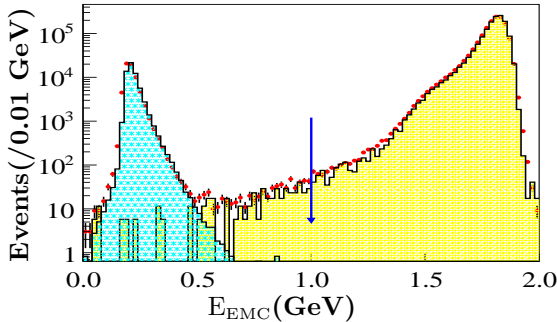


Fig. 1. The distributions of the deposited energies in the EMC of the charged tracks from the selected events, where the dots with red error bars are the continuum data, the yellow histogram is the Monte Carlo events of  $e^+e^- \rightarrow (\gamma)e^+e^-$  and the light green histogram is the Monte Carlo events of  $e^+e^- \rightarrow (\gamma)\mu^+\mu^-$ .

Figure 1 shows the deposited energies in the EMC ( $E_{EMC}$ ) for the good charged tracks of events satisfying the above selection criteria, where the dots with red error bars are the continuum data, the yellow histogram is  $e^+e^- \rightarrow (\gamma)e^+e^-$  Monte Carlo events and the light green histogram is  $e^+e^- \rightarrow (\gamma)\mu^+\mu^-$  Monte Carlo events. From the figure it can be seen that the requirement  $E_{EMC} > 1.0$  GeV can clearly separate the  $e^+e^- \rightarrow (\gamma)\mu^+\mu^-$  events from the Bhabha scattering events. To further remove background from cosmic rays, the momenta of the two good charged tracks in the candidate Bhabha events should not both be greater than  $E_b + 0.15$  GeV, where  $E_b$  is the calibrated beam energy.

After applying the above selection criteria, the accepted events are mostly Bhabha scattering events. But there may be still a small amount of background from  $e^+e^- \rightarrow (\gamma)J/\psi$ ,  $e^+e^- \rightarrow (\gamma)\psi(3686) \rightarrow (\gamma)J/\psi X$  and  $e^+e^- \rightarrow \psi(3770) \rightarrow (\gamma)J/\psi X$  ( $J/\psi \rightarrow e^+e^-$  and  $X = \pi^0\pi^0, \eta, \pi^0$  or  $\gamma\gamma$ ). In order to remove these background events, the sum of the momenta of the two good charged tracks is required to be greater than  $0.9 \times E_{cm}$ . The remaining contamination from these background sources

are estimated by Monte Carlo simulation, which will be discussed in Section 4.3.

### 4.2 Data analysis

The two oppositely charged tracks in the candidate Bhabha scattering events are bent in the magnetic field, so the positions of their two shower clusters in the xy-plane of the EMC are not back-to-back. To determine the observed number of Bhabha scattering events, we use the difference of the azimuthal angles of the two clusters in the EMC, which is defined as  $\delta\phi = |\phi_1 - \phi_2| - 180$  in degrees, where  $\phi_1$  and  $\phi_2$  are the azimuthal angles of the two clusters in the EMC. Figure 2 shows the  $\delta\phi$  distribution of the candidate Bhabha scattering events selected from the continuum data. In the figure, the events in the “signal” regions between the red arrows are taken as the signal events, while the ones in the “sideband” regions between the blue arrows are used to estimate the background in the  $\delta\phi$  “signal” region. After subtracting the scaled number of the events in the sideband region from the number of events in the signal region, we obtain the numbers of the Bhabha scattering events observed from data, which are listed in the second row of Table 1.

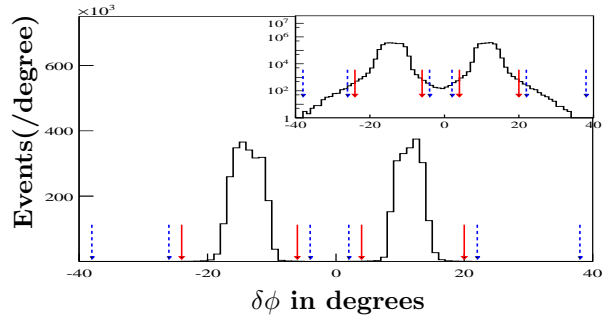


Fig. 2. The distribution of  $\delta\phi$  ( $\delta\phi = |\phi_1 - \phi_2| - 180^\circ$ ) of the selected  $e^+$  and  $e^-$  tracks.

### 4.3 Background estimation

For the accepted Bhabha scattering events, there may still be some residual background from  $e^+e^- \rightarrow (\gamma)J/\psi$ ,  $e^+e^- \rightarrow (\gamma)\psi(3686) \rightarrow (\gamma)J/\psi X$  and  $e^+e^- \rightarrow \psi(3770) \rightarrow (\gamma)J/\psi X$  ( $J/\psi \rightarrow e^+e^-$  and  $X = \pi^0\pi^0, \eta, \pi^0$  or  $\gamma\gamma$ ), as well as some other hadronic decay processes. These are estimated by analyzing the Monte Carlo events, including 16.5 M  $e^+e^- \rightarrow (\gamma)J/\psi$ , 51 M  $e^+e^- \rightarrow (\gamma)\psi(3686)$ , 198 M  $e^+e^- \rightarrow \psi(3770) \rightarrow D\bar{D}$ , 15 M  $e^+e^- \rightarrow \psi(3770) \rightarrow \text{non-}D\bar{D}$ , and 183 M  $e^+e^- \rightarrow \text{continuum light hadron events}$ . Detailed analysis gives the contamination rates to be  $\eta = 1.7 \times 10^{-5}$  and  $1.7 \times 10^{-4}$  for the candidate Bhabha scattering events selected from the continuum data and the  $\psi(3770)$  data, respectively.

#### 4.4 Detection efficiency for $e^+e^- \rightarrow (\gamma)e^+e^-$

To determine the detection efficiencies for the Bhabha scattering events, we generate 400,000  $e^+e^- \rightarrow (\gamma)e^+e^-$  Monte Carlo events with the Babayaga generator [4] within the polar angle range of  $|\cos\theta| < 0.83$  at  $\sqrt{s} = 3.650$  and  $3.773$  GeV, where  $\theta$  is the polar angle of the  $e^+$  and  $e^-$ . By analyzing these Monte Carlo events with the same selection criteria as the data analysis, we obtain the detection efficiencies for  $e^+e^- \rightarrow (\gamma)e^+e^-$  at  $\sqrt{s} = 3.650$  and  $3.773$  GeV, which are summarized in the fourth row of Table 1.

#### 4.5 Integrated luminosities

Inserting the numbers of observed Bhabha scattering events, the detection efficiencies for  $e^+e^- \rightarrow (\gamma)e^+e^-$

obtained by the Monte Carlo simulation, the trigger efficiency and the visible cross sections within the polar angle range of  $|\cos\theta| < 0.83$  in Eq. (2), we determine the integrated luminosities of the continuum data, the  $\psi(3770)$  data A and the  $\psi(3770)$  data B to be  $(44.49 \pm 0.02 \pm 0.44)$   $\text{pb}^{-1}$ ,  $(927.67 \pm 0.10 \pm 9.28)$   $\text{pb}^{-1}$  and  $(1989.27 \pm 0.15 \pm 19.89)$   $\text{pb}^{-1}$ , respectively, where the first errors are statistical and the second are systematic and discussed in the next section. The total luminosity of the  $\psi(3770)$  data is  $(2916.94 \pm 0.18 \pm 29.17)$   $\text{pb}^{-1}$ . Here, for the data sets used in the analysis, the trigger efficiency for collecting  $e^+e^- \rightarrow (\gamma)e^+e^-$  events was determined to be  $\epsilon_{e^+e^-}^{\text{trig}} = 100\%$  with the statistical error being less than 0.1% [3]. The numbers used in the luminosity measurements are summarized in Table 1.

Table 1. Summary of the numbers used in the determination of the luminosities, where  $N_{e^+e^- \rightarrow (\gamma)e^+e^-}^{\text{obs}}$  is the number of candidate Bhabha scattering events selected from the data,  $\epsilon$  is the detection efficiency,  $\sigma$  is the visible cross section for the Bhabha scattering events and  $L$  represents the integrated luminosity.

Samples	$\psi(3770)$ data A	$\psi(3770)$ data B	continuum data
$N_{e^+e^- \rightarrow (\gamma)e^+e^-}^{\text{obs}} (\times 10^4)$	$8412.9 \pm 0.9$	$18140.3 \pm 1.3$	$432.0 \pm 0.2$
$\eta (\times 10^{-4})$	1.7	1.7	0.17
$\epsilon$ (%)	61.28	61.62	61.47
$\sigma$ [nb]	147.9599	147.9599	157.9393
$L$ [ $\text{pb}^{-1}$ ]	$927.67 \pm 0.10 \pm 9.28$	$1989.27 \pm 0.15 \pm 19.89$	$44.49 \pm 0.02 \pm 0.44$

#### 4.6 Systematic error

In the measurements of the integrated luminosities, the systematic errors arise from the uncertainties associated with the Bhabha event selection, the Monte Carlo statistics, the background estimation, the signal region selection, the trigger efficiency and the generator.

In order to estimate the systematic uncertainty due to the  $\cos\theta$  requirement, we also determine the integrated luminosities with the selection requirements of  $|\cos\theta| < 0.75$  and  $0.70$ , and the differences from the standard selection of  $|\cos\theta| < 0.80$  are all less than 0.5% for both the continuum data and  $\psi(3770)$  data. To be conservative, we take 0.75% as the systematic error due to the  $\cos\theta$  selection in this work. The systematic uncertainty due to the MDC measurement information, which includes the uncertainties due to the MDC tracking efficiency and the momentum requirement, is determined to be 0.3% by comparing the integrated luminosities measured with and without the MDC measurement information. The systematic uncertainty due to the  $E_{EMC}$  energy selection requirements is determined to be 0.2%, by comparing the  $E_{EMC}$  distributions of the data and Monte Carlo events. The uncertainty from the  $E_{EMC}$  cluster reconstruction is determined to be 0.03% by comparing the efficiencies of the data and the Monte Carlo events.

The uncertainty from the Monte Carlo statistics is

0.1%. The uncertainty in the background subtraction is negligible. The uncertainty due to the  $\delta\phi$  signal region selection is estimated to be 0.01% by comparing the integrated luminosities measured with different signal regions. In these measurements, we use the trigger efficiency for collecting  $e^+e^- \rightarrow (\gamma)e^+e^-$  events of  $\epsilon_{e^+e^-}^{\text{trig}} = 100\%$  with the statistical error being less than 0.1% [3]. Therefore, we take 0.1% as the systematic uncertainty due to trigger efficiency. The uncertainty due to the Bhabha generator is 0.5%, which is cited from Ref. [4].

Table 2. The relative systematic uncertainties in the luminosity measurement.

Sources	$\Delta^{\text{sys}}$ (%)
$ \cos\theta  < 0.80$	0.75
$E_{EMC}^+ > 1$ GeV	0.2
$E_{EMC}^- > 1$ GeV	0.2
MDC information	0.3
EMC cluster reconstruction	0.03
Monte Carlo statistics	0.1
Background estimation	0.0
Signal region selection ( $\delta\phi$ )	0.01
Trigger efficiency [3]	0.1
Generator [4]	0.5
Total	1.0

Table 2 summarizes the above systematic uncertain-

---

ties in the luminosity measurement. The total systematic error is determined to be 1.0% by adding these uncertainties in quadrature.

## 5 Summary

By analyzing the Bhabha scattering events, we measure the integrated luminosities of the data taken at  $\sqrt{s} =$

3.650 and 3.773 GeV with the BESIII detector to be  $(44.49 \pm 0.02 \pm 0.44) \text{ pb}^{-1}$  and  $(2916.94 \pm 0.18 \pm 29.17) \text{ pb}^{-1}$ , respectively. These luminosities can be used in normalization in studies of  $\psi(3770)$  production and decays, as well as in studies of  $D$  meson production and decays.

*The BESIII collaboration thanks the staff of BEPCII and the computing center for their strong support.*

---

## References

- 1 BESIII Collaboration, M. Ablikim *et al.*, Design and construction of the BESIII detector, Nucl. Instrum. Meth. **A 614** (2010) 345.
- 2 BES Collaboration, J. Z. Bai *et al.*, Nucl. Instrum. Meth. **A 344** (1994) 319; Nucl. Instrum. Meth. **A 458** (2001) 627.
- 3 Trigger efficiencies at BES-III, N. Berger, Zhu Kai *et al.* Chinese Physics **C 34(12)** (2010) 1779-1784.
- 4 C.M. Carloni Calame, G. Montagna, O. Nicrosini, F. Piccinini, Nucl. Phys. Proc. Suppl. **131** (2004) 48-55.